

The Novosibirsk reservoir hydrothermal regime model*

V.V. Kravtchenko, E.N. Golubeva, A.A. Tskhai,
M.A. Tarhanova, M.V. Kraineva, G.A. Platov

Abstract. In this paper, the adaptation of the SibCIOM three-dimensional thermodynamic model is considered that allows modeling a three-dimensional velocity and temperature distribution, as well as a two-dimensional field of the ice cover for the Novosibirsk reservoir with seasonal changes in the water level. An analysis of the numerical results shows that the simulated processes, such as the main directions of the currents, seasonal changes in the basin water temperature and the dynamics of the average thickness of the ice cover, do not differ from that of the real processes characteristic of the Novosibirsk reservoir.

Keywords: Novosibirsk reservoir, three-dimensional thermodynamic model, the local one-dimensional ice model.

1. Introduction

The Novosibirsk reservoir is the largest artificial lake in West Siberia. It was created primarily as the power generation but it has played and continues to play an important role in the regional economy in many other ways. Various studies of hydrological, hydrochemical and hydrobiological processes for the reservoir during the period of its formation and later have been conducted [1]. Also, the regular monitoring of the water quality is carried out. The complex ecological monitoring is very important because of a great role of the reservoir in the operational regulation of the region energy supply, in the operational regulation of extremely uneven runoff of the Ob River throughout a year, in the water supply for population, agriculture and industry of the Novosibirsk Region and Altai Territory.

There are very important issues for the Novosibirsk reservoir like a significant drop in the water level during the winter period, the erosion of shores, bottom siltation and waterlogging shallow water. Because of shallow depth of intake pipes of large water intakes for water supply in the town of Berdsk and the urban-type settlement of Ordynskoye a significant water level drop can result in their stoppage. Also, this can cause shallow backwaters freezing and fish death. The main reasons of this phenomenon are the increased

*Supported by RFBR under Grant 18-41-220002 and in accordance with Government Order 0315-2019-0004.

water consumption at upstream and downstream areas and the increased outflow to downstream aimed at normal functioning of the urban water intakes and maintaining navigable depths. According to the project, the erosion of shores might have stopped after 40 or 50 years but, because of a large area of the lower reservoir part and the wind rose, the process continues. The protection is possible only by the way of building the shore protection structures like the natural analogues: a sandy beach or a stone talus.

Based on the above-said, many model problems arise concerning the Novosibirsk reservoir. Important parts of such problems are hydrodynamic and thermodynamic numerical models. The objective of this study is to construct a three-dimensional thermodynamic model that would consider the seasonal atmospheric changes, fluctuations in the water level due to unequal inflow and outflow. The system of the water condition research of the region in question is based on the 3D numerical hydrothermodynamic model SibCIOM developed at the Institute of Computational Mathematics and Mathematical Geophysics of the Siberian Branch of the Russian Academy of Sciences. This model is designed for studying the ocean and offshore sea water circulation [2].

2. Statement of the problem

From the town of Kamen-na-Obi up to the hydroelectric power station (HPS) dam the Novosibirsk reservoir is rather a narrow elongated body of water of about 200 km long (Figure 1). Conditionally, the Novosibirsk reservoir is divided into the three parts [1]. The lower part begins at the HPS dam and ends near to the village of Zavyalovo. It is a lake-like water body strictly stretched from south-west to north-east. Its length is 65 km, the widest part is 22 km and the deepest area is 25 km at the flooded bed near the dam. There are numerous isles in the left part of the submerged floodplain. The middle part begins near the village of Zavyalovo and ends near to the village of Ust-Aleus. It is a narrow part of the reservoir of about 100 km long and about 4 km wide. There are also some small isles along the left bank. The upper part begins near the village of Ust-Aleus and ends near to the town of Kamen-na-Obi. It is a strictly stretched from south to north water body of 35 km long. After creating the reservoir, the Ob floodplain was flooded, as a result, many large and small isles formed. This part is shallow, it has flooded shores.

The upper part was only partially included into the model domain, since by the moment, the model has not supported a sufficiently detailed description of the bottom topography and the many complex small-scale processes that arise in such an inhomogeneous region. Therefore, further in this study, the reservoir will be divided into the upper river-like and the lower lake-like parts.

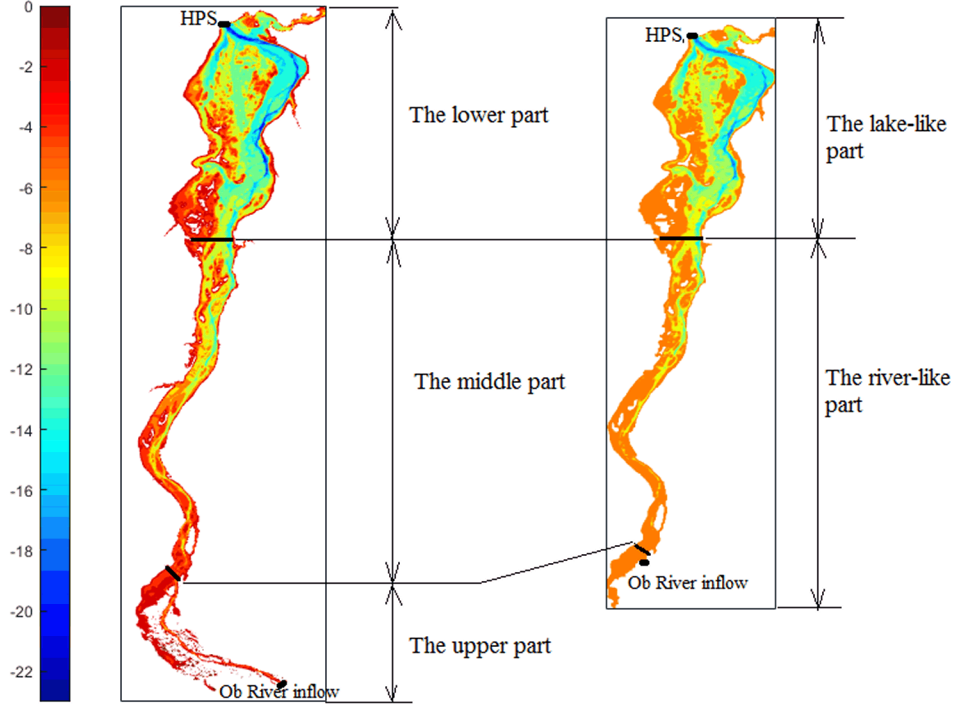


Figure 1. The Novosibirsk reservoir bottom topography during the top water level period — the topography based on the numerical relief model developed at the IWEP SB RAS (left) and the approximated one used for the numerical model simulation described in the paper (right)

In the Cartesian coordinate system x_1, x_2, z , where the axis z is vertically down, and in the domain Ω bounded by the shore line Γ_0 with the free surface level $\eta(x_1, x_2)$ and the reservoir bathymetry $H(x_1, x_2)$, we consider nonlinear hydrothermodynamic equations. The quasi-static approximation and the Boussinesq approximation are used:

$$\begin{aligned} \frac{\partial u}{\partial t} + L(u) - lw &= -\frac{1}{\rho_0} \frac{\partial p}{\partial x_1} + \frac{\partial}{\partial z} \nu_v \frac{\partial u}{\partial z} + F(u, \mu_v), \\ \frac{\partial v}{\partial t} + L(v) + lu &= -\frac{1}{\rho_0} \frac{\partial p}{\partial x_2} + \frac{\partial}{\partial z} \nu_v \frac{\partial v}{\partial z} + F(v, \mu_v), \\ \frac{\partial p}{\partial z} &= \rho g, \quad \frac{\partial u}{\partial x_1} + \frac{\partial v}{\partial x_2} + \frac{\partial w}{\partial z} = 0, \\ \frac{\partial T}{\partial t} &= L(T) + \frac{\partial}{\partial z} \nu_T \frac{\partial T}{\partial z} + F(T, \mu_T). \end{aligned}$$

Here (u, v, w) is the velocity vector, T is the water temperature, p is the pressure, ρ is the density calculated from the equation of state $\rho = \rho(T, p)$,

ρ_0 is the average density, $l = 2\Omega \sin \varphi$ is the Coriolis parameter, φ is the latitude, μ_v, ν_v and μ_T, ν_T are the coefficients of horizontal and vertical viscosity and diffusion, respectively. The transfer operator L and the diffusion operator F are the following:

$$L(\phi) = \frac{\partial}{\partial x_1}(u\phi) + \frac{\partial}{\partial x_2}(v\phi) + \frac{\partial}{\partial z}(w\phi),$$

$$F(\phi, \mu) = \left[\frac{\partial}{\partial x_1} \left(\mu \frac{\partial \phi}{\partial x_1} \right) + \frac{\partial}{\partial x_2} \left(\mu \frac{\partial \phi}{\partial x_2} \right) \right].$$

At the initial time instant there is some initial state u^0, v^0, T^0 . The boundary conditions at the free surface level $z = \eta(x_1, x_2)$ are the following:

- the momentum flux is caused by the surface wind stress (τ_{x_1}, τ_{x_2})

$$-\nu_v \left(\frac{\partial u}{\partial z}, \frac{\partial v}{\partial z} \right) = \frac{(\tau_{x_1}, \tau_{x_2})}{\rho_0};$$

- the vertical velocity is calculated from the condition $w = \frac{\partial \eta}{\partial t}$;
- the heat flux is calculated from the relation

$$-\nu \frac{\partial T}{\partial z} = C(T_S - T_A) \sqrt{u^2 + v^2} \quad \text{or} \quad -\nu \frac{\partial T}{\partial z} = F_T,$$

where T_S, T_A are the surface temperature and the atmosphere temperature, respectively, and C is the empirical constant. In the second case, F_T is determined in the course of the operation of the additional local 1D ice model.

The boundary conditions at the reservoir bottom $z = H(x_1, x_2)$ are the following:

- the flow condition

$$w = u \frac{\partial H}{\partial x_1} + v \frac{\partial H}{\partial x_2},$$

- the quadratic bottom friction condition

$$\nu \left(\frac{\partial u}{\partial z}, \frac{\partial v}{\partial z} \right) = -C_D \sqrt{u^2 + v^2} \cdot (u, v),$$

- the zero heat flux through the reservoir bottom

$$\vec{N}_H \cdot \text{grad } T = 0,$$

where C_D is the empirical dimensionless constant, \vec{N}_H is the external normal to the bottom surface.

The solid boundary conditions on shore line Γ_0 and isles boundaries Γ_i , $i = \overline{1, N}$, are the zero horizontal velocity components and the zero heat flux

$$u = 0, \quad v = 0, \quad \vec{n} \cdot \text{grad } T = 0,$$

where \vec{n} is the external normal to the vertical boundary.

The fluid boundaries conditions are described below.

For the instant convection mixing caused by the reservoir surface cooling, the additional procedure based on the assessment of the water reservoir stratification sustainability is used.

In case of the negative surface temperature, the ice model is triggered. For the interaction of the atmosphere and the thermodynamic part the local 1D ice model [3, 4] and the parameter values from the AOMIP website [5] are used. In the model, ice is represented as a motionless solid plate with the temperature linear distribution along the vertical coordinate. Then the heat flux through the ice Q_i is calculated as

$$Q_i = C_i \frac{T_i - T_f}{h},$$

where C_i is the empirical constant, T_f is the freezing point of water, T_i is the ice surface temperature, h is the ice thickness.

The ice growth at the ice-water boundary is calculated from the heat balance

$$\rho_i L_f \varphi_{iw} = Q_f + Q_w + Q_i,$$

where φ_{iw} is the changing rate of the ice thickness at the lower boundary, ρ_i is the ice density, L_f is the ice latent heat, Q_w is the heat flux from water to ice calculated as

$$Q_w = C_w |\vec{v}| (T_f - T_w),$$

T_w is the water surface temperature, C_w is the empirical constant, \vec{v} is the horizontal velocity of the water flow.

The ice forms when water has cooled to a freezing point. If the calculated water temperature of the water column drops below freezing, it is restricted to value of T_f and the difference is taken as an additional heat flux from the water to the ice

$$Q_f = \frac{\partial}{\partial t} \int_0^{z_0} \rho c_{pw} (T_f - T_w) dz,$$

$Q_f = 0$ in other cases. Here c_{pw} is the water heat capacity.

The unknown temperature of the ice surface can be determined from the heat balance at the atmosphere-ice boundary:

$$Q_a = Q_i,$$

where Q_a is the heat flux from the atmosphere.

If the calculated temperature T_i exceeds the melting point of ice T_{mi} , then it is assumed $T_i := T_{mi}$.

The ice growth rate φ_{ai} at the atmosphere-ice boundary is calculated from the heat balance

$$\rho_i L_f \varphi_{ai} = -Q_a - Q_i.$$

So, the total rate of a change in the ice thickness is $\varphi = \varphi_{iw} + \varphi_{ai}$, and $\int_{t^n}^{t^{n+1}} \varphi dt$ is a change in the ice thickness over the time $[t^n, t^{n+1}]$.

Also, the heat flux F_T , that is used as the boundary condition for the heat equation, is calculated as

$$F_T = \begin{cases} \frac{Q_a}{c_{pw}\rho} & \text{in the open water,} \\ -\frac{Q_w}{c_{pw}\rho} & \text{in the water covered with ice.} \end{cases}$$

Two versions of determining the atmosphere heat flux were considered. In the first case, the heat flux is equal to a sensible heat flux based on the atmosphere temperature and wind speed:

$$Q_a = C_a |\vec{u}_{wind}| (T_a - T_i).$$

In the second case, the atmosphere heat flux is the sum of the sensible heat flux F_S , the latent heat flux F_L , the incoming shortwave radiation F , and the outgoing longwave radiation R .

The turbulent fluxes of the sensible and latent heat are calculated by the integrated aerodynamic formulas

$$\begin{aligned} F_S &= c_{pa} \rho_a \text{St} V_a (T_i - T_a), & F_L &= L \rho_a \text{Da} V_a (q_i - q_a), \\ q_i &= \frac{0.622 e_i}{p_a - 0.378 e_i}, & q_a &= \frac{0.622 e_a}{p_a - 0.378 e_a}, \\ e_i &= 10^{\tau_i}, & \text{where } \tau_i &= \frac{0.7859 + 0.03477 T_i}{1 + 0.00412 T_i} + 0.00422 T_i + 2. \end{aligned}$$

Here q_a , e_a , T_a , p_a , and V_a are the specific atmosphere humidity, the water vapor tension (daily-averaged observations from the weather station on the isle of Dalniy [6]), the atmosphere temperature (daily-averaged observations from the weather station on the isle of Dalniy), the atmosphere pressure

(at the moment it is constant and equal to 750 mm of mercury), and the wind speed (daily-averaged observations from the weather station on the isle of Dalniy), respectively; e_i is saturated vapor pressure corresponding to the temperature of 0°C, q_i is the ice surface specific humidity; c_{pa} is the air heat capacity at constant pressure; St , Da are the Stanton number and the Dalton number, respectively; and L is the heat of sublimation.

The shortwave and longwave radiations are determined by the formulas

$$R = \varepsilon\sigma(T_i + 273.15)^4(0.39 - 0.005\sqrt{e_a})(1 - 0.8c_f) + 4\varepsilon\sigma(T_i + 273.15)^3(T_i - T_a),$$

$$F = F_0(1 - 0.6c_f^3)(1 - \alpha),$$

$$F_0 = \frac{S \cos^2(z_\theta)}{(\cos(z_\theta) + 2.7)e_a \cdot 10^{-5} + 1.085 \cos(z_\theta) + 0.1},$$

where σ is the Stefan–Boltzmann constant, c_f is the relative cloud cover, ε is the surface emissivity, F_0 is the incoming shortwave radiation for the clear sky, α is the underlying albedo, S is the solar constant, and z_θ is the solar zenith angle.

3. Numerical model

The approximation grid with a horizontal spacing of 113 m is used for the numerical model. The vertical grid has the basic spacing of 1 m bellow a fixed depth. The upper layer spacing is allowed to vary in vertical (Figure 2). This grid can be reduced to the uniform one with the help of the vertical variable replacement

$$\sigma = \frac{z - z_b}{\eta - z_b},$$

where z_b is the fixed depth.

According to the Agreement of November 15, 2017 between the Institute of Water and Environmental Problems SB RAS and the Institute of Computational Mathematics and Mathematical Geophysics SB RAS, the numerical relief model developed in the IWEP SB RAS is used for constructing the approximate bathymetry in the model. This bathymetry is the step function whose constant values are the closest along the vertical coordinate to the corresponding grid points.

The solid boundary is formed by the shore line and big isles boundaries. The fluid boundaries are the Ob and the Berd Rivers inflow and outflow in the HPS area, respectively.

For the numerical tests, the data based on the real climate data are used for constructing the initial and boundary conditions. These are the 1981 year observational data from the weather station on the isle of Dalniy, that indicate to the average daily atmosphere temperature, the prevailing wind

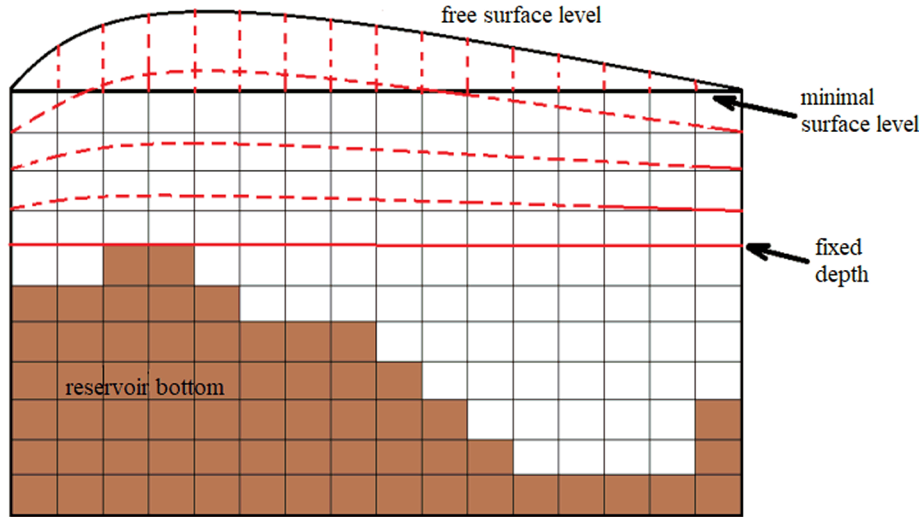


Figure 2. Schematic representation of a vertical grid in the numerical model

direction and speed, the water vapor tension and the cloud cover [6]; the hydrological data for the Ob and the Berd Rivers such as inflow average values, water temperature and free surface level [7] (Figures 3 and 4), and outflow over the HPS area. The atmosphere data are used for impulse and heat fluxes calculation at the reservoir surface. The hydrological data are used as fluid boundary conditions for the water velocity and temperature.

As the initial temperature distribution, a vertically uniform field with the temperature equal to the winter temperature is considered. The time step of the model is equal to 5 minutes.

Let us consider in greater detail the specification of initial and boundary conditions for a free surface. Since we know the value of the level only at the beginning of the reservoir (see Figure 4), this is rather a difficult task. Using only these data as the boundary condition brings about the incorrect statement of the problem. There is an approach to the iterative calculation of an approximate water level value in the HPS area with the help of data at the beginning of the reservoir. The method is a gradual correction of the outflow rate so that the calculated level values are close to the known data at the beginning of the reservoir [1].

In this paper, we use another method based on the inflow/outflow balance and the assumption that during the year there is no excess of the extreme values such as the dead storage level (108.5 m BS) and the top water level (113.5 m BS). In our case, the correction is such that the initial value is chosen so that a minimum water level corresponds to the dead storage level, and the water level calculated in the model is considered to be unchanged in the region of the HPS, when the value exceeds the value cor-

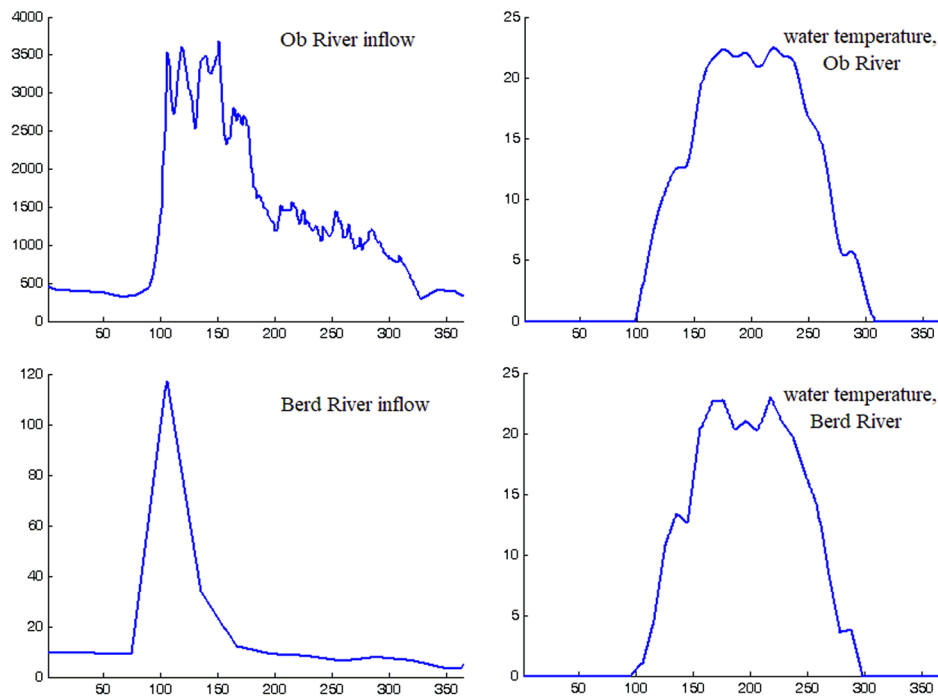


Figure 3. Inflow and water temperature data for the Ob River (upper images) and for the Berd River (lower images)

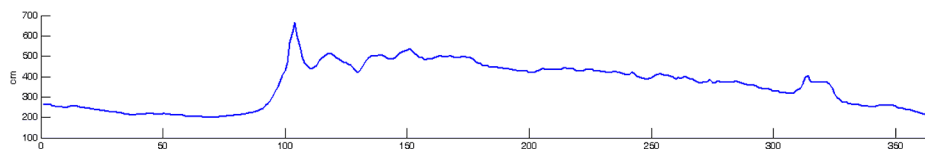


Figure 4. Water level data at the beginning of the Novosibirsk reservoir near the town of Kamen-na-Obi

responding to the top water level. Thus, the correction of the level is carried out at the expense of an additional discharge through the HPS, but from the results obtained (Figure 5) it can be seen that the additional discharge occurs during the period from the end of May up to the beginning of June, when, probably, there is an additional discharge through the spillway dam.

The fact that the hydrological observational data may contain a significant error is also indicated by an approximate estimate of the water level based on the inflow/outflow balance (Figure 6). This can be seen after a year has passed that there is a significant accumulation of water volume non-typical of the object under study. In case of the correction of the water level, the calculated result is close in its form to the natural regime of the reservoir with a minimum in mid-April, followed by a sharp rise whose speed

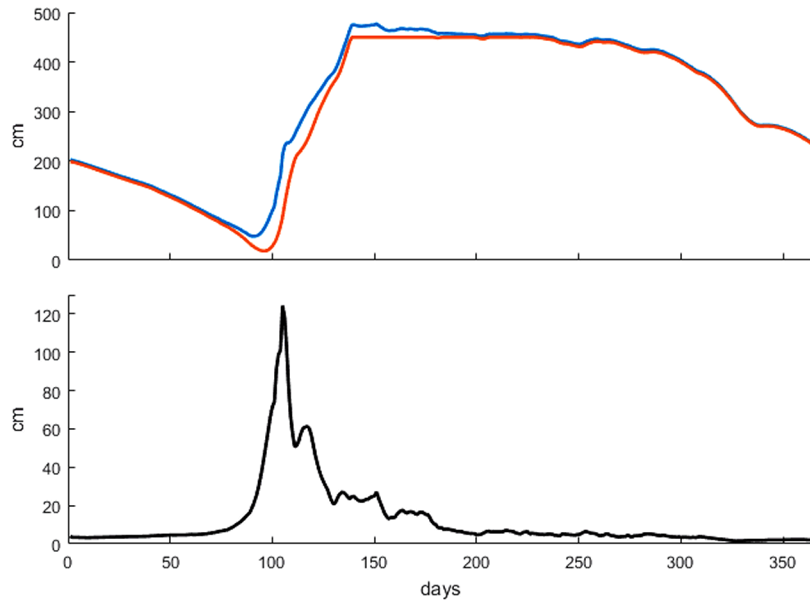


Figure 5. The results of the water level calculation in the model: upper graph — water level fluctuations during the year near the HPS (red line) and near the beginning of the river part of the reservoir (blue line), lower graph — the difference between the level values in the upper and lower parts of the reservoir

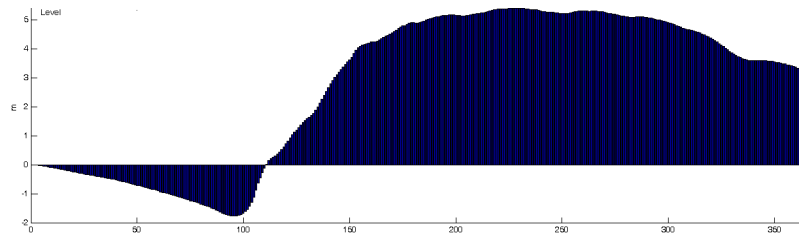


Figure 6. An approximate estimate of a change in the water level based on the daily-averaged inflows (the data on the Ob and the Berd Rivers) and the daily-averaged outflow (the data on discharges through the HPS)

depends on the passage of the flood wave, almost constant in the summer period and a gradual decrease in the autumn period.

4. Numerical results

The most important processes that determine the temporal variability of the state of the region waters include the summer heating, the autumn-winter cooling, the ice formation and its melting. In this regard, one-dimensional calculations of the thermal state of water and ice were carried out for a

time period equal to two estimated years using the data on the state of the atmosphere for 1981. The periods of the ice formation and melting and the seasonal variation of the temperature of the reservoir were analyzed in various options for defining the heat fluxes on the reservoir surface. The calculation results are presented in Figures 7 and 8. The calculations done have shown that a more powerful heating of the reservoir occurs in the numerical calculations when determining the heat flux on the surface of a

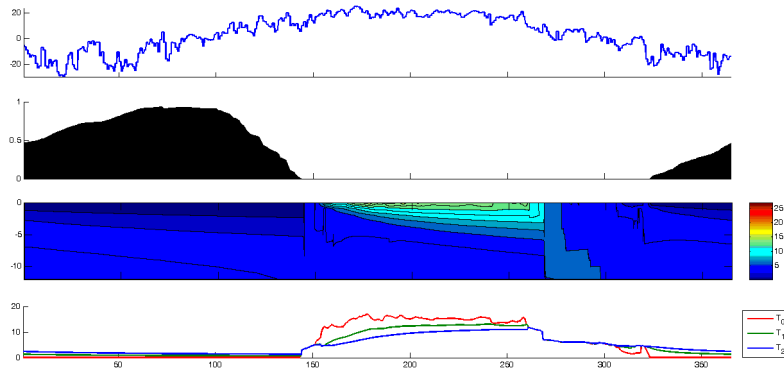


Figure 7. The result of calculating a seasonal variation of the temperature in the reservoir and the thickness of the ice during the second simulated year according to the results of the one-dimensional version of the model. The calculation of surface heat fluxes is based on atmospheric temperature and wind speed. The panels from top to bottom are: the seasonal variability in the daily-averaged temperature of the lower atmosphere ($^{\circ}\text{C}$); the variability in the ice thickness (m); the vertical variability in the temperature distribution ($^{\circ}\text{C}$) (depth in meters); and temperature change at the surface (T_0) and at a depth of 1 m (T_1) and 2 m (T_2)

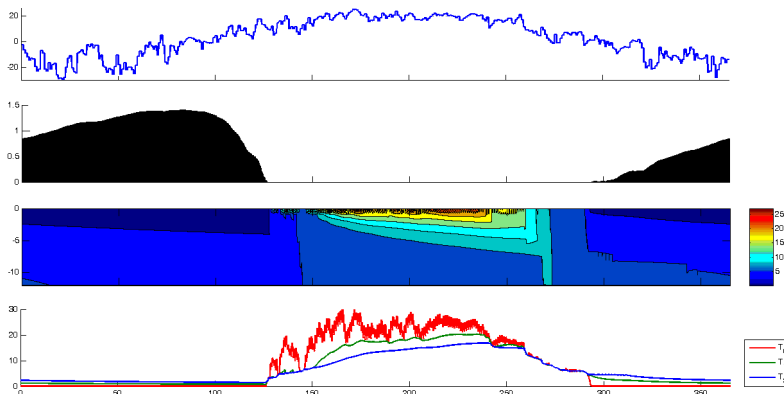


Figure 8. The same as Figure 7, but the calculation of surface heat fluxes was carried out with allowance for additional latent heat fluxes and components of the radiation balance

reservoir based on the extended list of components, which includes shortwave and longwave radiations and a latent heat flux, than that which takes into account only the temperature of the atmosphere and the wind speed.

It is also worth noting that seasonal changes in the second case are caused not only by a change in the atmospheric temperature, but also with variability in the rate of evaporation from the surface and with changes in the intensity and duration of the daily insolation associated with astronomic seasonality.

The numerical calculation for the basic three-dimensional model for establishing the seasonal variation was carried out for a period of two years. The data for each of both two years were taken in accord with the 1981 observational data.

The numerical model forms three-dimensional fields of temperature, current velocity, and two-dimensional fields of ice thickness and water level height. The daily-averaged calculated data were recorded into the archive and were made suitable for further analysis.

The model presented reproduces the autumn-winter cooling of the reservoir and the formation of an almost uniform water structure. Between November and March, the reservoir is covered with ice, whose thickness reaches 1.4 m. This is slightly higher than the multiyear-average value of approximately 1.0 m, obtained from the observations, but is at the level of the observed maximum. It is worth noting that at the moment the model does not fully take into account the effect of thermal insulation due to the snow cover.

At the beginning of April, the Ob River water begins to flow into the region with a positive temperature, which contributes to the onset of intense ice melting in the shallow region (below 6 m) under the condition of a positive atmosphere temperature. The gradual warming of the reservoir water, associated with the spread of the river tributary, continues passing down along the reservoir. However, at the beginning of May most of the reservoir remains covered with ice (Figure 9). More intense melting of the ice is characteristic of the right bank of the reservoir, in accord with the former location of the main river bed. The complete release from ice in this experiment occurs in mid-May.

In the subsequent period, heating of the surface waters continues (Figure 10). Due to intense currents, the active mixing takes place in the river part of the reservoir. In its lake part, with a slight wind, the underlying layers gradually warm up with forming a pronounced stratification of waters. But the situation can dramatically change in the case of an increase in the north-north-east wind (exceeding 3.5 m/s), which can cause a shift in the flow pattern and intense mixing (Figure 11).

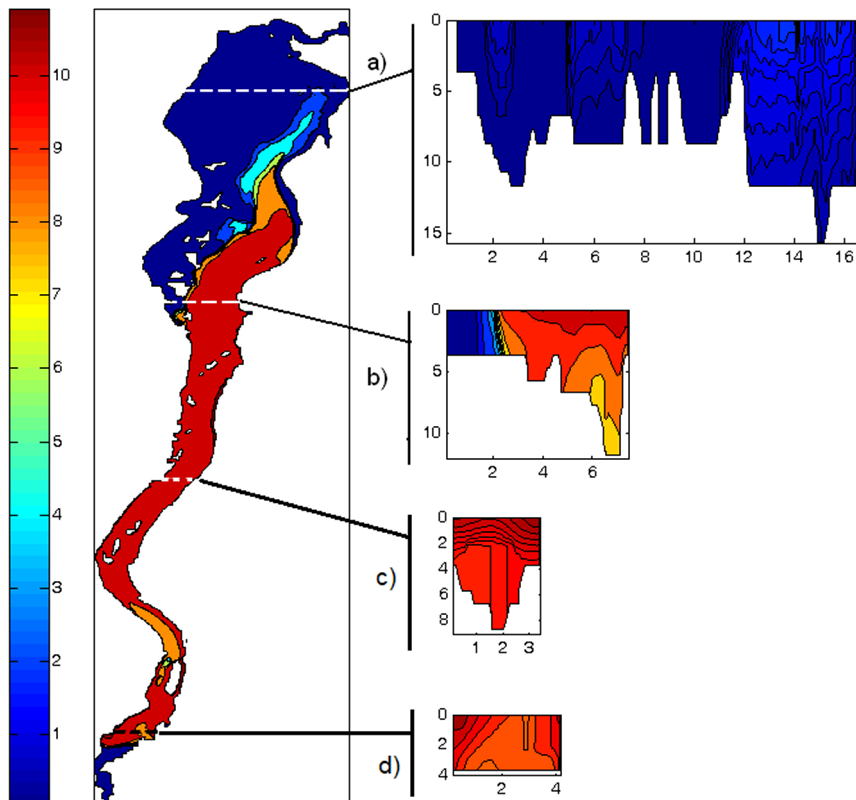


Figure 9. The start of the warming up period. In the early May, according to the simulation results, most of the reservoir is covered with ice (blue color). On the right is the temperature ($^{\circ}\text{C}$) on the reservoir surface. On the left are the vertical sections of the temperature field (depth in meters, width in kilometers). Sections go through the lake part (a), near the village of Zavyalovo (b), near the urban-type settlement of Ordynskoye (c), and near the village of Ust-Aleus (d)

The cooling of the reservoir begins in August and ends by the third decade of October. Figure 12 shows the beginning of the destruction of the stratification in the lake part caused by the surface water cooling. Figure 13 shows the temperature field corresponding to October 17. The river part of the reservoir is still affected by the warmth of the Ob River, but a relatively uniform temperature of 3–5 degrees Celsius has been already established in the lake part.

In the flow pattern of the reservoir, the main current transporting the water of the Ob and the Berd Rivers towards the HPS is simulated. In winter, the dynamic impact of the atmosphere is eliminated due to the formation of the ice cover, the water circulation is determined by the main direction of the flow of the incoming water and the topography of the

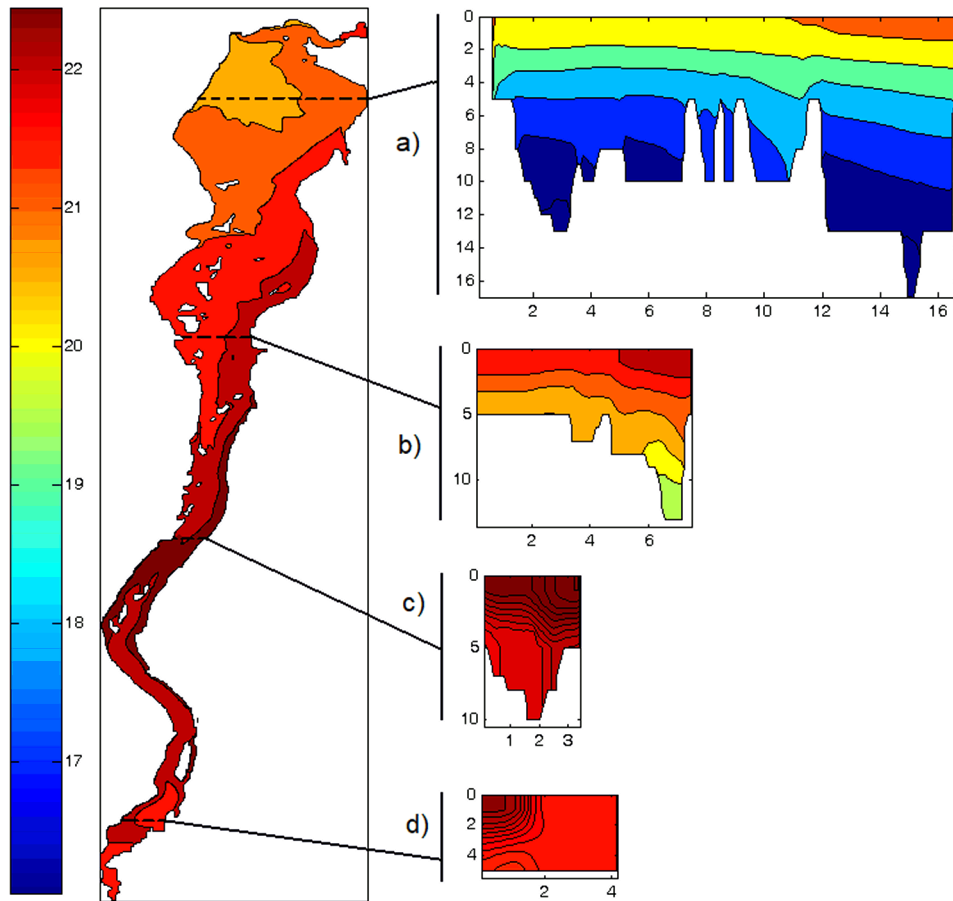


Figure 10. The reservoir temperature in mid-June. An almost uniform temperature field in the river part. Gradual warming up of the lake part with steady summer stratification

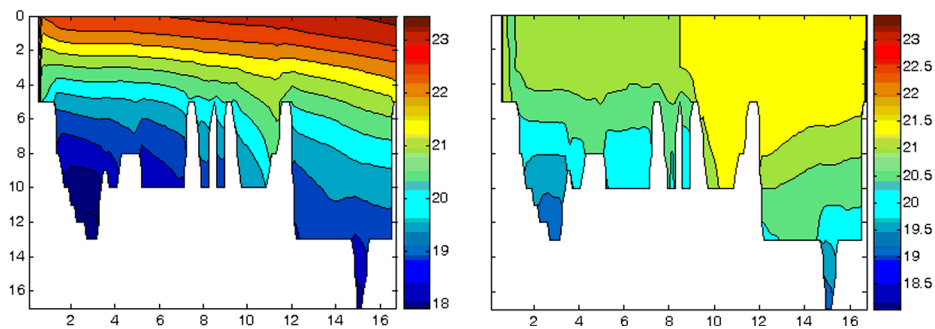


Figure 11. The destruction of stable stratification after an event of wind amplification. The vertical temperature section in the widest part of the reservoir. On the left — June 20, 1981 (North wind, 1.4 m/s), on the right — June 25, 1981 (North-North-East wind, 4.5 m/s)

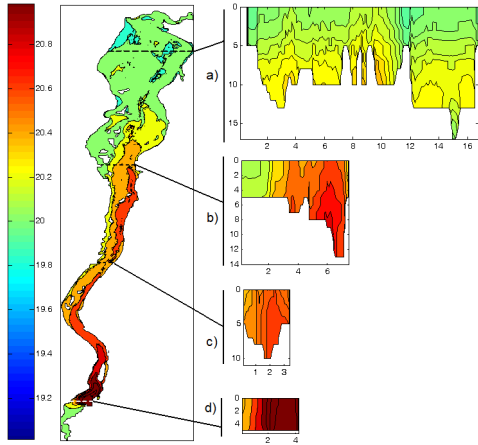


Figure 12. Mid-August. The beginning of the cooling of the reservoir

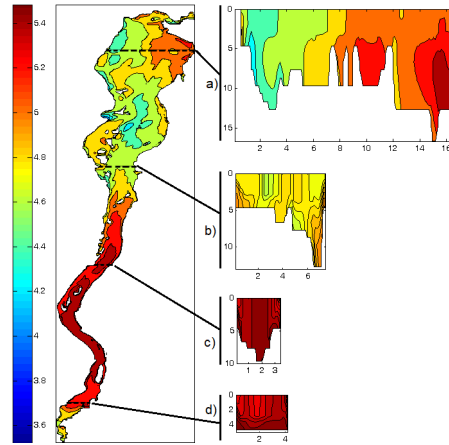


Figure 13. The end of the autumn cooling process

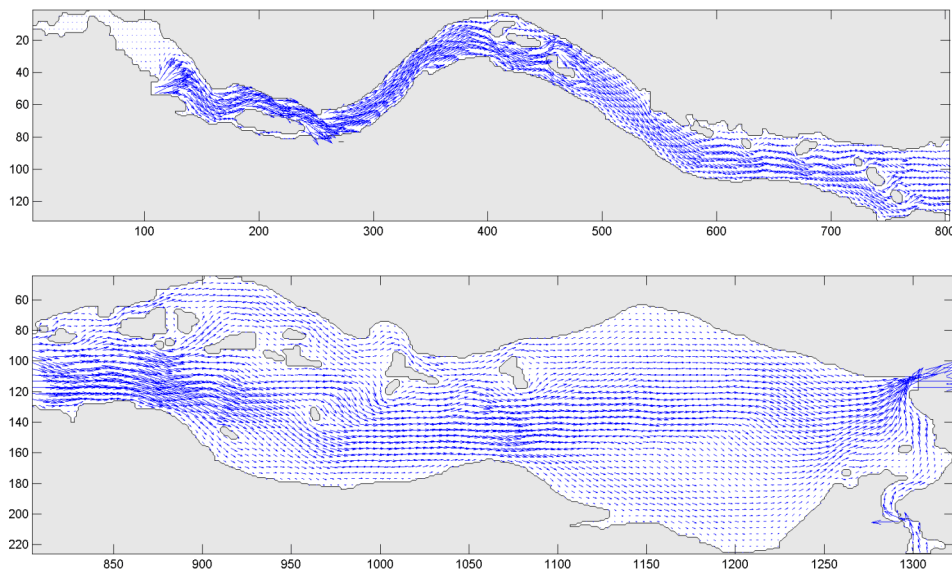


Figure 14. Currents in the surface layer (2 m) in winter. Above is the river part, below is the lake part

reservoir. In this regard, the flow pattern is notable for its considerable stability during the winter period (Figure 14).

When the surface is set free from ice in the spring-summer period, a strong influence on the distribution of currents is exerted by the wind field, due to which a shift of the main current can occur. Some versions of the flow pattern for the spring-summer period are presented in Figures 15 and 16.

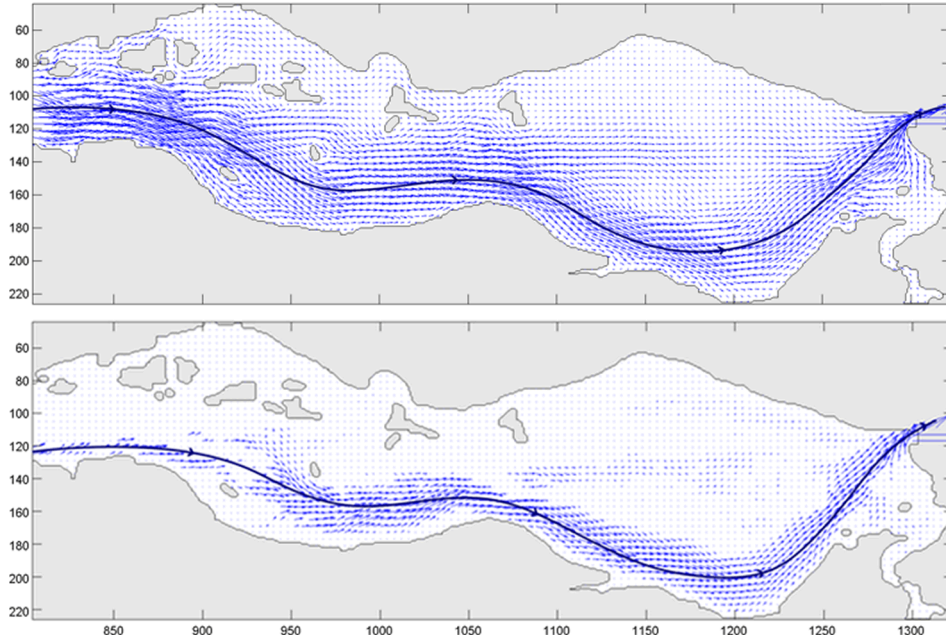


Figure 15. A flow pattern for May 20, 1981 (the upper panel presents 2 m depth, the lower panel—10 m)

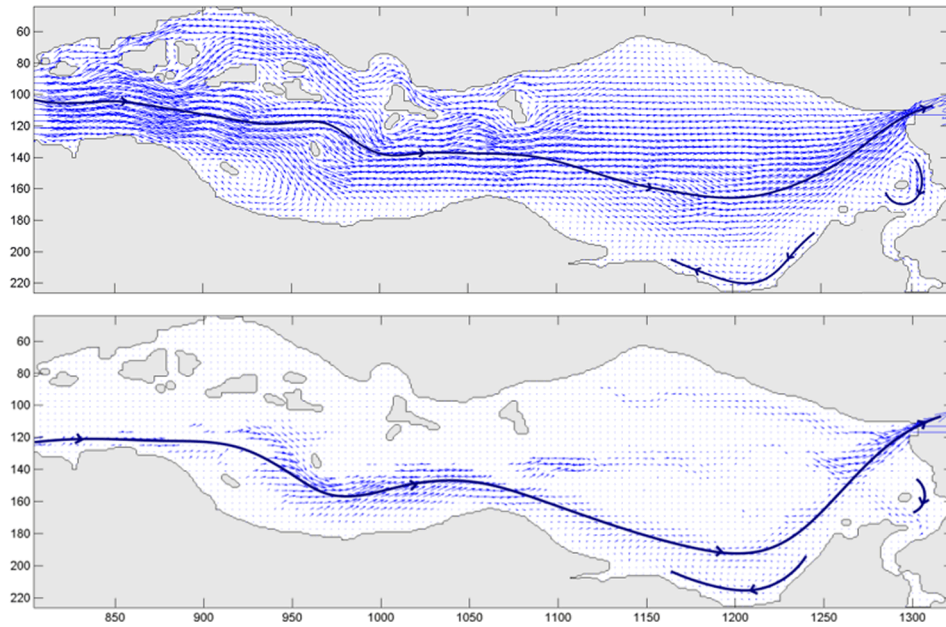


Figure 16. The flow pattern for June 20, 1981 (the upper panel presents 2 m depth, the lower panel—10 m)

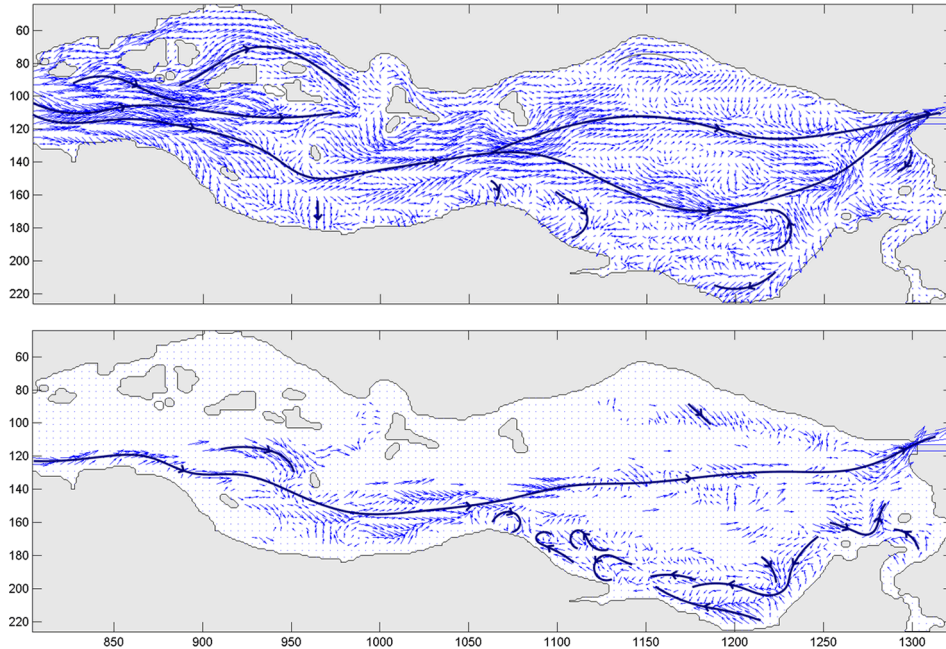


Figure 17. The flow pattern for September 20, 1981 (the upper panel presents 2 m depth, the lower panel – 10 m)

The autumn cooling brings about the activation of the reservoir convective mixing, which leads to the forming irregular structures in the flow pattern in addition to the main current (Figure 17).

5. Concluding remarks

The adaptation of the SibCIOM three-dimensional thermodynamic model allows the simulation of a three-dimensional velocity and temperature distribution, as well as a two-dimensional field of the ice cover for the reservoir with seasonal changes in the water level. An analysis of the numerical results shows that the simulated processes, such as the main directions of the currents, seasonal changes in the basin water temperature and the dynamics of the average thickness of the ice cover, do not differ from that of the real processes characteristic of the Novosibirsk reservoir [1].

The currents in the upper part of the reservoir have the characteristics of a river system with a fairly narrow channel and shallow depths. The formation of the flow pattern in this part is mainly influenced by the volume of water coming from the Ob River and the bottom topography. In the lower lake part of the reservoir (from the village of Zavyalovo up to the dam of the hydroelectric power station), these factors are the main ones in the formation

of the flow only in the winter period, when the water column under the ice layer is almost uniform in temperature (about 1 degree Celsius) and it is not exposed to wind. When the surface of the water is ice-free, the main stream may shift under the influence of the wind, and in the case of the autumn cooling, when there is a sharp cooling of surface waters, activation of convective mixing of the water mass leads to the emergence of many irregular structures in the general flow pattern.

According to the test results of the three-dimensional model the first ice appears in late October. The ice setting ends by mid-November. The upper part of the reservoir is released from the ice due to the entry of the Ob River warm water. In the lower part of the reservoir, the ice remains until mid-May.

Additionally, regarding thermodynamics, we can say that in the period of the ice-free water, the river part is characterized by an almost uniform temperature field, determined mainly by the temperature of the waters coming from the Ob River. Closer to the lake part, as the flow velocity decreases, the influence of the heat flux from the surface becomes more noticeable. In the lake part, in the absence of strong winds of the north-north-east directions and sharp fluctuations in the air temperature, there is a gradual heating or cooling of the waters with the formation of stable stratification. Otherwise, an intense mixing occurs until the formation of an almost uniform distribution.

Further development is assumed to improve the ice model, and to achieve a more adequate way to set the boundary and initial conditions for the water level.

Based on a locally one-dimensional ice model test, it was shown that the surface water heating and seasonal ice changes are closer to real values if the calculation of the total heat flux includes shortwave and longwave radiations and a latent heat flux. However so far, the current model has not taken into account the influence of snow cover, as well as the result of the autumn-winter runoff of the reservoir with a decrease in the water level.

The determination of the initial and boundary conditions for the water level is complicated by a currently simplified relief, both in terms of taking into account the topography of shallow water and in terms of taking into account the geographic elevation in

the river part of the reservoir. It is also difficult to assess the error of observations. Therefore, at the moment, a simple way to correct the boundary conditions is based on the calculated inflow/outflow balance.

In general, it can be noted that the model proposed, even in a simplified version, makes it possible to simulate the seasonal variability of the Novosibirsk reservoir water state.

References

- [1] Savkin V.M. et al. Long-Term Dynamics of Water and Ecological Regime of Novosibirsk Reservoir. — Novosibirsk: Publishing House of SB RAS, 2014.
- [2] Golubeva E.N., Platov G.A. On improving the simulation of Atlantic Water circulation in the Arctic Ocean // *J. Geophys. Res.* — 2007. — Vol. 112. — C04S05. doi:10.1029/2006JC003734.
- [3] Platov G.A. The investigation of the sea-ice model thermodynamic regimes // *Bull. Novosibirsk Comp. Center. Ser. Numerical Modeling in Atmosphere, Ocean, and Environment Studies.* — Novosibirsk, 1996. — Iss. 4. — P. 53–66.
- [4] Bukatov A.E., Zavyalov D.D., Solomakha T.A. Thermal evolution of the sea ice in the Taman and the Dinsk bays // *Morskoy Gidrofizicheskiy Jurnal.* — 2017. — No. 5. — P. 21–34 (In Russian).
- [5] The Arctic Ocean Model Intercomparison Project. — <http://www.whoi.edu> (reference date: 20.11.2018).
- [6] Complex Studies of the Novosibirsk Reservoir / Yu.I. Podlipskiy, Yu.I. Chaikovskaya, eds. — Moscow: Gidrometeoizdat, 1985 (In Russian).
- [7] The State Water Cadaster. Annual Data about Regime and Resources of Surface Land Waters. Part 1. — 1981. — Vol. 1, No. 10. (In Russian).

